Energy Conversion and Management 249 (2021) 114841

Contents lists available at ScienceDirect

Energy Conversion and Management

journal homepage: www.elsevier.com/locate/enconman

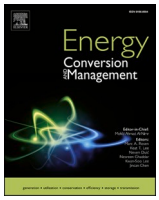

Evaluation of hybrid evaporative-vapor compression air conditioners for different global climates

Tabeel A. Jacob *, Nihar Shah, Won Young Park

Energy Analysis and Environmental Impacts Division, Lawrence Berkeley National Laboratory, Berkeley, United States

ARTICLE INFO

Keywords:
Evaporative cooling
Air-conditioning
Climate assessment
Energy efficiency
Cooling efficiency

ABSTRACT

Currently, a majority of global residential air-conditioning requirements are met using cooling systems based on the vapor compression cycle (VCC). To meet the future demand for space cooling and to reduce the corresponding environmental impact, there is a need for alternative cooling systems which require less resources and exhibit a higher coefficient of performance (COP). One of proposed alternatives is called the hybrid evaporative-vapor compression (HEVC) cycle, which utilizes adiabatic latent cooling in combination with the VCC. In this paper, we conducted a feasibility analysis of a HEVC system by comparing its performance to that of VCC for various global climates. To accomplish this, we developed and validated models to simulate the performance of residential VCC and HEVC systems. ASHRAE weather data and design conditions were then used to compare the performance of the two systems. In general, HEVC systems are best suited for hot arid climates with energy reduction greater than 20%. Conversely, humid climates are not suitable for HEVC adoption due to degraded performance of evaporative coolers in these climates. In addition to comparing the energy savings from HEVC systems, it is also critical to analyze their water consumption. Generally, climates that benefit the most from HEVC technology tend to also experience water scarcity issues. Thus, both the energy savings and water consumption of HEVC systems must be analyzed to guide the discussion on their adoption.

1. Introduction

Rapid urbanization and rising temperatures from anthropogenic climate change have led to a significant increase in the demand for space cooling technologies. This growth, if left unabated, will significantly increase global energy consumption and the need for more power generation. According to a projection by the International Energy Agency (IEA) [1], commercial and domestic space cooling will account for 37% of the global electricity demand by 2050. The IEA report [1] also highlights the urgency in improving the energy efficiency of our existing air-conditioning technology. For example, a twofold increase in energy efficiency of the current market average may result in a 45% lower global cooling energy demand in 2050. A recent survey of the global air conditioning market reveals that the average efficiency of the air-conditioners being currently being sold is less than half compared to the top-tier expensive air-conditioning products [2].

Currently, a majority of our existing domestic air-conditioning needs are met using a relatively mature and well-understood technology called vapor compression cycle (VCC) [3,4]. Generally, the equipment based on VCC has been optimized to the point where further efficiency improvements require a significant increase in their cost. The compression work for these systems is comparatively high. This is especially the case for hot and dry climates, where the standard VCC systems experience a significant efficiency penalization due to high condenser temperatures and consequently, higher compression power requirements. Past research on the topic indicates that the coefficient of performance (COP) of these systems decreases by 2–4% for every 1 °C increase in the condenser temperature [5].

While many alternative technologies (such as ejector enhanced VCC, VCC with multi-stage compression, VCC with suction-line heat exchanger, etc. [6,7]) are being explored, hybrid evaporative-vapor compression (HEVC) systems are a promising low-cost energy efficient alternative to standard VCC air-conditioners [8–12]. Pre-cooling of outdoor air through an evaporative cooler attached to a VCC system lowers temperatures in the VCC condenser, and consequently, enables the VCC system to operate more efficiently by reducing the compression work.

Although HEVC is an attractive low-cost cooling technology, it is critical to analyze the performance of HEVC systems for different climates and identify the climates which are best suitable for HEVC systems. During direct evaporative cooling, the wet bulb temperature does

* Corresponding author.
E-mail address: tjacob@lbl.gov (T.A. Jacob).

https://doi.org/10.1016/j.enconman.2021.114841
Received 2 July 2021; Accepted 30 September 2021
Available online 19 October 2021

Nomenclature

Symbols

A_{fr}	frontal area of the evaporative pad (m^2)
c_p	specific heat capacity (kJ $kg^{-1}K^{-1}$)
COP	coefficient of performance (–)
f	frequency (hz)
h	specific enthalpy (kJ kg^{-1})
ln	natural logarithm (–)
$\dot{m}$	mass flow rate (kg s^{-1})
P	pressure (kPa)
PR	ratio of discharge pressure over suction pressure in the VCC (–)
$\dot{Q}$	heat duty (kW)
s	specific entropy (kJ $°C^{-1}$ kg^{-1})
T	temperature (°C)
$\dot{W}$	power (kW)
WMO	World Meteorological Organization (–)

Greek Letters

α	heat transfer coefficient (kW m^{-2} K^{-1})
α_m	mass transfer coefficient (kg m^{-2} s^{-1})
Δx	segment length of the evaporative pad (m)
η_{evap}	saturation efficiency of the evaporative media (–)
η_s	isentropic efficiency of the VCC compressor (–)
η_{vol}	volumetric efficiency of the VCC compressor (–)
ω	specific humidity (kg kg^{-1})
ρ	density (kg m^{-3})
ξ	specific surface area of the evaporative pad (m^2 m^{-3})

subscripts

a	air
C	condenser
DB	dry bulb
E	evaporator
i	segment number
ref	refrigerant
SC	subcooling
SH	superheating
v	water vapor in air
w	make-up water in the evaporative cooler
WB	wet bulb

not change from the inlet to the outlet, and the dry-bulb temperature of the air may not be cooled below the wet-bulb temperature. Additionally, the rate of mass transfer during the evaporation process directly depends on the relative humidity of the outdoor air. Since hot dry air is able to absorb a relatively greater amount of moisture compared to cold humid air, implementing HEVC systems in humid climates will provide lower energy savings compared to hot and dry climates.

Furthermore, past laboratory-scale experimental investigations on HEVC often consider tap water as a "free resource" while assessing the feasibility of HEVC systems. However, many recent studies emphasize the importance of conserving freshwater [13]. Of particular concern is the nexus between water and energy production. Currently, an unsustainable amount of water is used for electricity production [14]. As the global population and energy demands continue to grow, the availability of water will become a significant issue and will affect our ability to generate energy [15]. Areas that would benefit most from HEVC systems are generally in hot and dry climates which also tend to experience water scarcity. Therefore, water should be treated as a critical resource and any new energy-saving solution must also consider the impact of its water usage on the global freshwater reserves.

Thus, in this paper, we investigated the feasibility of HEVC system by comparing its performance to that of VCC systems for 21 different global climates. The goal of this research is to identify the climates which are best suited for HEVC systems. The remainder of this paper is organized as follows. Section 2 gives a brief overview of the prior work on HEVC systems. Section 3 describes the methodology, data and assumptions we employed to develop our models. Using these models, we investigate the energy savings potential of utilizing low-cost residential HEVC systems and compare them to VCC systems. Section 4 discusses the analysis results and implications of our findings. Section 5 summarizes the conclusions.

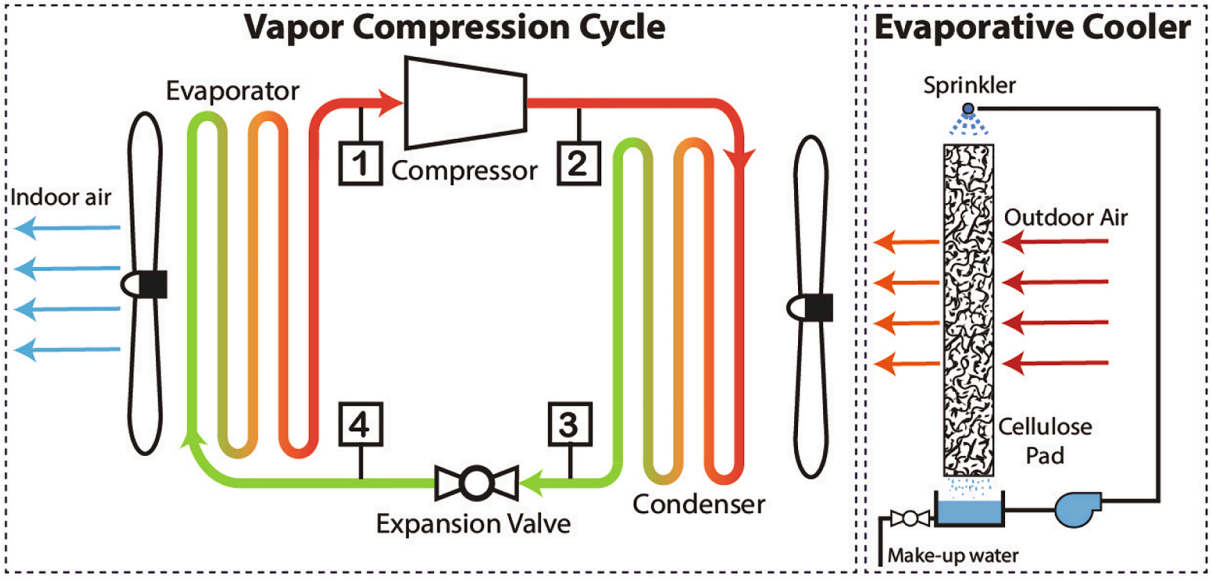

Fig. 1. A schematic of the hybrid evaporative-vapor compression system.

2. HEVC system overview and literature review

Fig. 1 shows a schematic of a HEVC system, which comprises of a standard VCC system and a direct evaporative cooler attached to the VCC condenser. A small pump is used to feed utility water at top of a porous evaporative media, which may be constructed out of low-cost materials such as cellulose, polyvinyl chloride (PVC), polyester, etc. The outdoor air flowing through the evaporative cooler undergoes adiabatic cooling as evaporation occurs on the surface of the evaporative media.

Fig. 2 shows a representative comparison of temperature-entropy diagrams for two cases at the same operating conditions; 1) a standard VCC and 2) an HEVC. Note, in this diagram, the condensation happens between state points 2 and 3. We observe that the pre-cooling of outdoor air using evaporative cooling results in lower temperatures in the condenser, and consequently, enables the VCC system to operate much more efficiently by reducing the compression work.

A review of the literature reveals several past analytical and experimental studies which investigate the benefits of incorporating evaporative cooling into VCC systems. Among the earliest investigations on the topic, Goswami et al. [16] retrofitted the condenser of an 8.8 kW air-conditioner with a 20.3 cm thick evaporative cooling pad and a re-circulating water pump (similar to the configuration shown in Fig. 1). They measured and compared the performance of the system with and without the evaporative cooler. The testing was conducted during the summer months in Gainesville (Florida, USA) where the climate classification according to Köppen-Geiger criteria is Cfa. Their experiments confirmed that pre-cooling the outdoor air using evaporative cooling resulted in a lower condenser pressure in the air-conditioner and consequently resulted in an approximately 17–20% reduction in compressor power consumption.

Hajidavalloo and Eghtedari [17] retrofitted a 5.3 kW split air-conditioner with a 5 cm thick cellulose pad. Testing was conducted for outdoor dry-bulb temperatures ranging from 35 to 49 °C and outdoor relative humidities ranging from 12 to 40%. They observed a COP enhancement ranging from 32 to 51% during the testing of HEVC system. The performance of HEVC system was less sensitive to changes in the outdoor dry-bulb temperature compared to the VCC system without the evaporative cooler. Additionally, the water consumption of the evaporative cooler ranged from 7 to 8.2 L/hr for the conditions investigated.

Similar superior performance of HEVC systems have been reported by other investigations on the topic [10,11,18,19]. These results suggest that hot and dry climates (classified as BSh, BSk, BWh, and BWk by the Köppen-Geiger criteria) will certainly benefit from the adoption of HEVC systems. However, it is important to note that a majority of the testing in the literature was conducted at relatively high outdoor dry-bulb temperatures (usually above 35°C and low relative humidities (usually below 40%). The trends from these studies may overpredict the performance of HEVC systems in cold and humid climates. Thus, there is need to investigate the performance of HEVC in all of the global climates. Such analysis is critical to guide future energy policy discussions and for identifying the most sustainable, environment-friendly space cooling technologies.

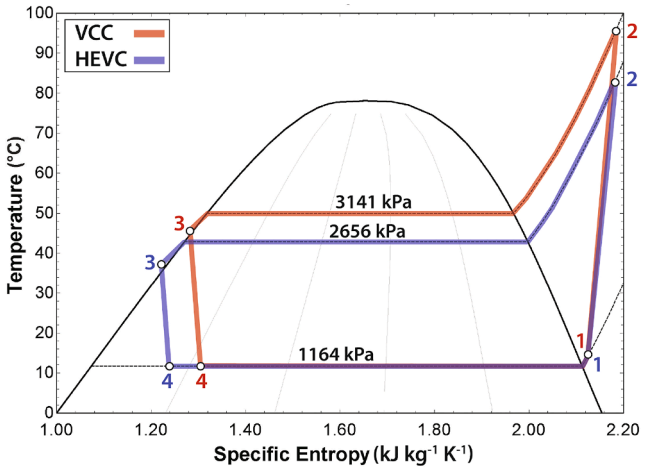

Fig. 2. Temperature versus specific entropy for both vapor compression cycle and hybrid evaporative-vapor compression systems. For both the cases, the outdoor dry bulb temperature and humidity were equal to 35 °C and 40%, respectively. The indoor dry bulb temperature was 26.7 °C. The modeling methodology is provided in Table 2.

3. Modeling approach

3.1. Climate conditions

Table 1 lists the climate classifications, along with the details of cities that were considered during this study. This analysis was conducted for twenty-one different climate conditions, based on the widely-cited Köppen-Geiger climate classifications [20]. To compare the performance of HEVC and VCC systems in these climates, thermodynamic models were developed for both configurations. For HEVC system, the annual rates of water consumption for different climates are also determined. These model estimate the energy consumption and cooling capacity of the system based on the ASHRAE weather data [21].

For each city, ASHRAE [21] provides monthly design conditions that are representative of the local weather for that month. These values were derived by conducting a temperature-bin analysis on the hourly weather data. The design temperatures are selected such that they statistically have a low probability of being exceeded. In the current study, the selected design temperatures correspond to a statistical 95% confidence interval. Additionally, there are two types of design conditions. The monthly design dry bulb and mean coincident wet bulb temperatures are used for processes that are driven by heat transfer with the ambient. Conversely, monthly design wet bulb and mean coincident dry bulb temperatures are more appropriate for applications with evaporative heat and mass transfer [21]. Thus, in the current study, the outdoor conditions for VCC and HEVC were set based on monthly design dry bulb and monthly design wet bulb temperatures, respectively. Fig. 3 shows a distribution of the design temperatures considered in this study.

3.2. Vapor compression system

To simulate the performance of a VCC, a thermodynamic state point model was developed using the Engineering Equation Solver (EES) program [22]. The approach followed here is summarized in Table 2 and is often employed in the literature to investigate VCC modifications, as well as for screening new refrigerants [3,7,23]. In particular, readers are referred to Domanski and McLinden [24] for an in-depth review of the different methods used to model vapor compression systems. In this model, the refrigerant-side pressure drop in the heat exchangers was assumed negligible. The dry bulb and wet bulb temperatures of the cooled space were set as 26.7 °C and 19.4 °C for all the simulations in this study, which is based on testing guidelines specified by the AHRI Standard 210/240 [25]. The condensation saturation temperature was assumed to be 15 °C higher than the outdoor air dry bulb temperature, while the evaporation temperature was assumed to be 15 °C lower than the indoor air dry bulb temperature. The superheat in the evaporator and subcooling in the condenser were set equal to 5 °C. Lastly, the expansion process in the expansion device was modeled as isenthalpic.

The compressor model was informed by our prior experimental testing of a fixed-speed 3.5 kW air-conditioner, with an EER equal to 3.5 W/W. The working fluid in the system was R32. Testing was conducted in the psychometric test chambers at Lawrence Berkeley National Lab and followed the procedure outlined by AHRI Standard 210/240 [25].

Table 1
List of cities considered in this study and their climate classification based on the Köppen-Geiger criteria [20,21].

Köppen-Geiger climate classification		Country	City	WMO station identifier	Elevation (m)	Annual cooling hours* (hr)
Af	Tropical (Rainforest)	Singapore	Paya Lebar	486940	20	15576
Am	Tropical (Monsoon)	Cameroon	Douala	649100	10	9738
As	Tropical (Savanna, dry summer)	India	Indore	427540	564	15338
Aw	Tropical (Savanna, dry winter)	USA	Key West	722010	1	8844
BSh	Arid (Hot steppe)	Pakistan	Lahore	416400	215	22860
BSk	Arid (Cold steppe)	USA	Denver	724690	1612	2111
BWh	Arid (Hot dessert)	USA	Phoenix	722780	337	25472
BWk	Arid (Cold dessert)	Iran	Isfahan	408000	1546	9543
Cfa	Temperate (No dry season, hot summer)	Italy	Milan	160800	108	1974
Cfb	Temperate (No dry season, warm summer)	France	Paris	071560	77	518
Csa	Temperate (Dry summer, hot summer)	USA	Sacramento	724830	5	4366
Csb	Temperate (Dry summer, warm summer)	USA	Seattle	727930	113	277
Cwa	Temperate (Dry winter, hot summer)	India	New Dehli	421820	215	21757
Cwb	Temperate (Dry winter, warm summer)	Mexico	Mexico City	766793	2230	317
Dfa	Continental (No dry season, hot summer)	Japan	Sapporo	474120	26	257
Dfb	Continental (No dry season, warm summer)	Canada	Montreal	716120	73	409
Dsa	Continental (Dry summer, hot summer)	USA	Salt Lake	725720	1288	4181
Dsb	Continental (Dry summer, warm summer)	USA	Lake Tahoe	725847	1925	243
Dwa	Continental (Dry winter, hot summer)	China	Beijing	545110	35	3353
Dwb	Continental (Dry winter, warm summer)	Russia	Khabarovsk	317350	75	448
Dwc	Continental (Dry winter, cold summer)	Russia	Chita	307580	693	488

* The annual cooling hours are based on reference temperature equal to 26.7 °C.

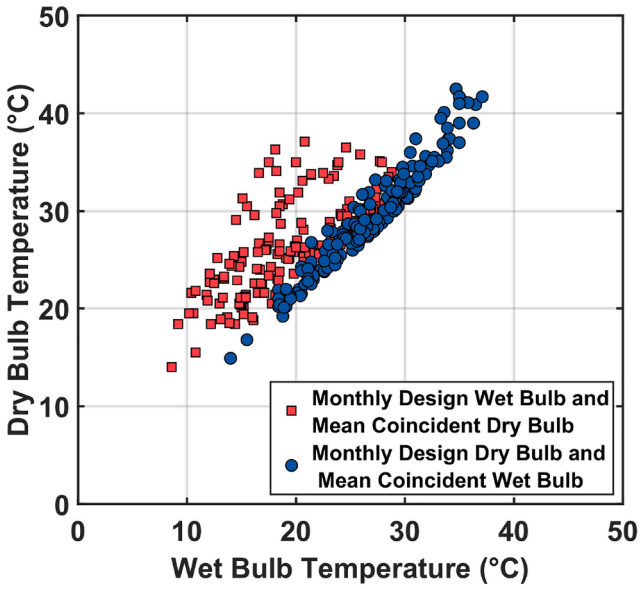

Fig. 3. Distribution of design dry bulb and wet bulb temperature for 21 different climates listed in Table 1. Data from 2017 ASHRAE Handbook: Fundamentals[21].

The measured data were first used to evaluate the isentropic and volumetric efficiencies during the operation of the system. Using a simple regression analysis, the isentropic efficiency of the compressor was then correlated to the pressure ratio in the system (discharge pressure divided by the suction pressure):

$$\eta_s = 0.764 - 0.0465PR \tag{1}$$

For a given pressure ratio, the isentropic efficiency and Eq. 2 can be used to determine the power consumption of the compressor.

$$W_c = \frac{\dot{m}_{ref}(h_{2,s} - h_1)}{\eta_s} \tag{2}$$

where $\dot{m}_{ref}$ and h_1 are the mass flow rate and suction enthlapy at the compressor inlet. $h_{2,s}$ is the isentropic discharge enthalpy evaluated at the discharge pressure and suction entropy.

Table 2
Modeling equations for the vapor compression cycle.

State	Description	Equation(s)
1	Evaporator outlet	$T_E = T_{DB,indoor} - 15°C$
		$T_{SH} = 5°C$
		$T_1 = T_E + T_{SH}$
		$P_1 = f(T_E)$
		$h_1 = f(P_1, T_1)$
		$s_1 = f(T_1, P_1)$
2	Compressor outlet	$T_2 = f(P_2, h_2)$
		$P_2 = f(T_C)$
		$h_{2,s} = f(P_2, s_1)$
		$h_2 = h_1 + \frac{\dot{W}_c}{\dot{m}_{ref}}$
3	Condenser outlet	$T_C = T_{DB,outdoor} + 15°C$
		$T_{SC} = 5°C$
		$T_3 = T_C - T_{SC}$
		$P_3 = P_2$
4	Expansion valve outlet	$T_4 = f(P_4, h_4)$
		$P_4 = P_1$
		$h_4 = h_3$
–	Cooling capacity	$\dot{Q}_E = \dot{m}_{ref}(h_1 - h_4)$
–	Power	$\dot{W} = \dot{W}_c + \dot{W}_{fan,indoor} + \dot{W}_{fan,outdoor}$
–	COP	$COP = \dot{Q}_E / \dot{W}$

$A = f(B)$ denotes that A is a function of B.

Similarly, the expression for volumetric efficiency of the compressor was experimentally determined to be:

$$\eta_{vol} = 1.091 - 0.0691PR \tag{3}$$

The actual refrigerant mass flux is then equal to the theoretical mass flow rate multiplied by the volumetric efficiency:

$$\dot{m}_{ref} = \dot{m}_{ref,theo}\eta_{vol} = (V_{displacement} f \rho_1)\eta_{vol} \tag{4}$$

where $V_{displacement}$, f and ρ_1 are the compressor volumetric displacement, compressor rotational speed (revolutions per second) and refrigerant suction density, respectively.

Finally, the total power consumption, cooling capacity, and system COP are evaluated using the relations presented in Table 2.

Experimental testing of HEVC and VCC systems by Martinez et al. [10] suggests that the addition of evaporative cooling pad may not significantly affect the power consumption of the outdoor fan. Therefore, to simplify the analysis in this paper, the power consumption of the indoor fan and outdoor fans were assumed to be constant equal to 30 W and 60 W for both HEVC and VCC systems.

3.3. Evaporative cooler

The heat and mass transport phenomena during evaporative cooling have been studied extensively in the past literature [26–30]. An in-depth review of the modeling methods and assumptions revealed that there was lack a of agreement between these studies. Consequently, their conclusions differed as well. Therefore to simulate evaporative cooling for this study, we used an understanding of first principles as well as the findings from the literature to develop a discretized 1-dimensional model. We made the following assumptions to simplify the analysis:

1. The process is adiabatic and the heat transfer between the surrounding is considered negligible.
2. The temperature and relative humidity of the humid air are uniform in all planes, except for the plane parallel to the airflow i.e. 1D model.
3. The water distribution on the evaporative media is uniform.
4. The inlet temperature of the make-up water is equal to the outdoor wet bulb temperature.
5. The convective heat and mass transfer coefficients are constant throughout the evaporative media.

Fig. 4 shows a schematic of the evaporating cooling process. The evaporative media was discretized in the direction parallel to the air flow, with thickness Δx. In the model, the pad thickness and segment thickness were set equal to 100mm and 5mm, respectively. This resulted in a total 20 segments. For each segment, the air mass balance can be expressed as:

$$\dot{m}_{a,i} = \dot{m}_{a,i+1} \tag{5}$$

where i denotes the segment number. Similarly, the water mass balance can be written as:

$$\dot{m}_{w,i} = \dot{m}_{v,i+1} - \dot{m}_{v,i} = \dot{m}_{a,i}(\omega_{i+1} - \omega_i) \tag{6}$$

where $\dot{m}_{w,i}, \dot{m}_v$ and ω are the mass of evaporated water in segment i, the mass of water vapor in the air and air humidity ratio, respectively.

The energy balance in the segment i can be written as:

$$\dot{Q}_i = \dot{m}_{a,i}\left[\left(h_{a,i+1} + h_{v,i+1}\omega_{i+1}\right) - \left(h_{a,i} + h_{v,i}\omega_i\right)\right] + \dot{m}_{w,i}h_w \tag{7}$$

where h_a, h_v and h_w are the enthalpies for air, water vapor and make-up water, respectively. $\dot{Q}_i$ is the heat absorbed due to evaporative cooling, which can also be expressed in terms of the convective heat transfer coefficient, α:

$$\dot{Q}_i = \xi A_{fr}\Delta x\alpha\frac{\left(T_{a,DB,i} - T_w\right) - \left(T_{a,DB,i+1} - T_w\right)}{ln\frac{\left(T_{a,DB,i} - T_w\right)}{\left(T_{a,DB,i+1} - T_w\right)}} \tag{8}$$

where ξ and A_{fr} are the specific surface area and frontal area of the evaporative pad. Corrugated cellulose was selected as the material of construction for the evaporative media due to its widespread adoption in the evaporative cooling industry. Specifically, we considered the product with the commercial name CELdek7060, which has a specific surface area equal to 363 m^{-2} m^{-3}. The convective heat transfer coefficients were evaluated from the correlation suggested by He et al. [30], who systematically investigated the performance of evaporative cooling using cellulose and polyvinyl chloride (PVC) pads.

For air–water mixtures, the Lewis number is approximately equal to one [21]. Therefore, an analogy exists between the mass and heat transfer which can be used to evaluate the mass transfer coefficient, α_m:

$$\alpha_m = \frac{\alpha}{\rho c_p} \tag{9}$$

With a known mass transfer coefficient, the rate of water evaporated is equal to:

$$\dot{m}_{w,i} = \xi A_{fr}\Delta x\alpha_m(\omega_{sat} - \omega_i) \tag{10}$$

where ω_{sat} is the humidity ratio of the saturated water vapor.

Finally, Eqs. (5)–(10) are solved iteratively for each segment to determine the temperatures, humidity ratio, and heat duties for the whole evaporative pad. Additionally, the rate of water evaporated is equal to the sum of $\dot{m}_{w,i}$ in all segments.

The resulting trends predicted by the evaporative cooler model are presented in Fig. 5a and b. Fig. 5a shows that the saturation efficiency (Eq. 11) decreases with an increase in the air velocity. This is primarily

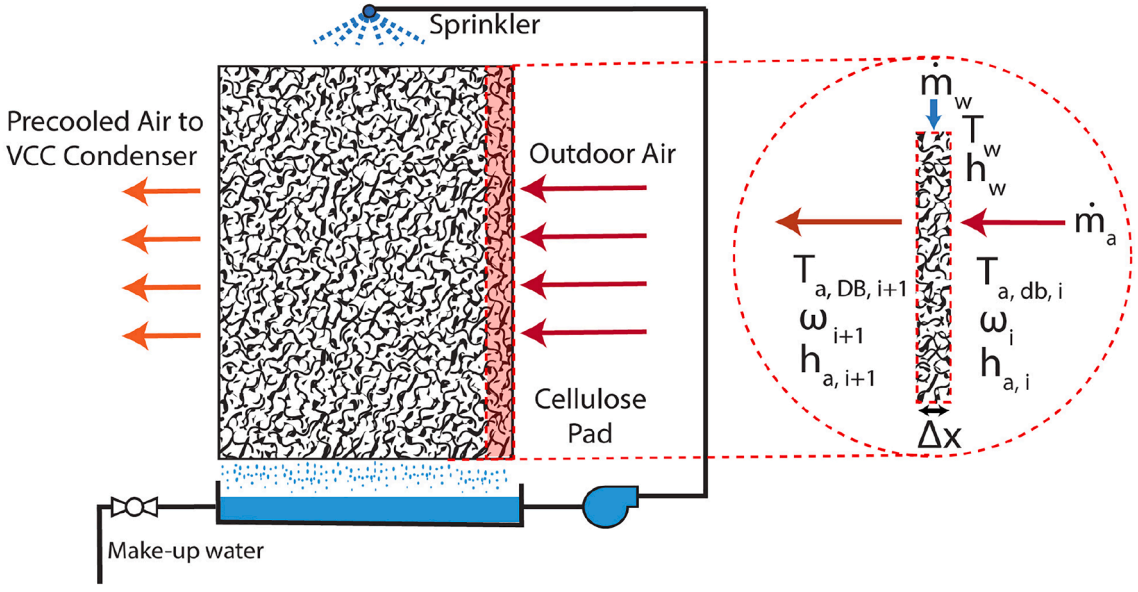

Fig. 4. A schematic of the evaporative cooler.

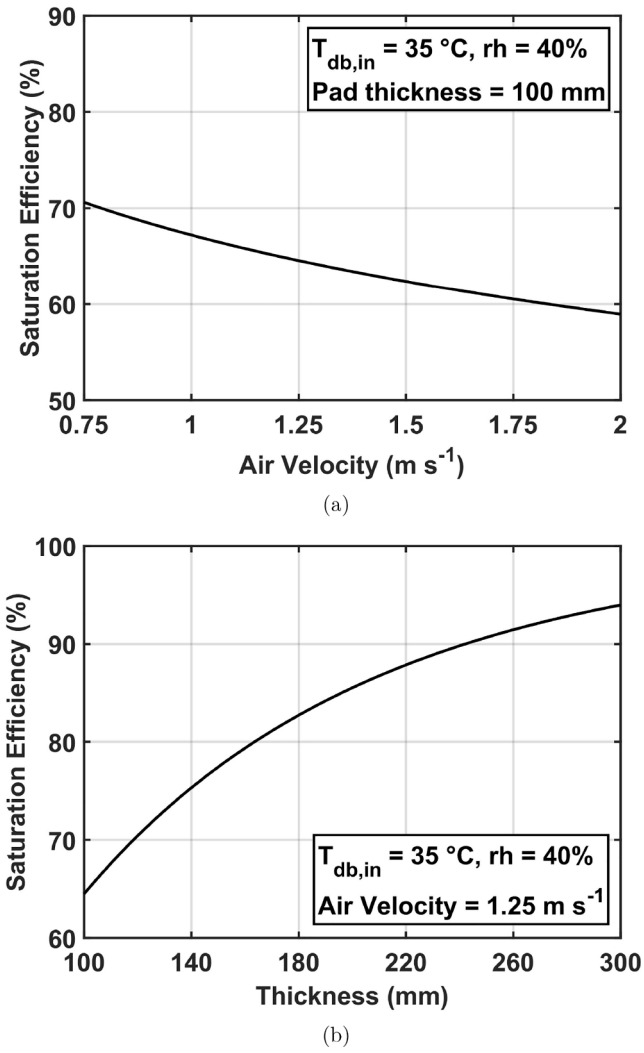

Fig. 5. Results from the evaporative cooling model: (a) Air velocity versus saturation efficiency (b) Pad thickness versus saturation efficiency.

due to relatively shorter residence times for higher velocity flows. As result, the mass and heat transfer rates are inhibited. Increasing the pad thickness has the opposite effect, as it increases the amount of surface area and time available for air to exchange heat and mass. However, the air-side pressure drop also increases with increasing evaporative media thickness and must also be considered during the design of an evaporative cooler. The trends predicted described above are consistent with experimental observations from past studies [30,10,26]

$$\eta_{evap} = \frac{T_{DB,in} - T_{DB,out}}{T_{DB,in} - T_{WB}} \times 100\% \quad (11)$$

To further gain confidence in the accuracy of the model described above, we compared its predictions to the experimental data collected by Martínez et al. [10] during evaporative cooling. Martínez et al. [10] measured the airflow rates, inlet temperatures, and outlet temperatures for three cellulose pads with varying thicknesses. Table 3 shows the parameters that were adjusted in our model to mimic their experimental setup. Fig. 6(a) and (b) show the measured dry bulb temperatures and saturation efficiencies compared against the predictions from our model, respectively. The average outlet dry bulb temperature deviation was equal to −0.14 °C. The predicted saturation efficiencies were on average 2.5% higher than measured values. Overall, the agreement was good which provided us confidence in the modeling methodology of the evaporative cooler.

Table 3
Input parameters used to model evaporative cooling: Validation (1st Column) and analysis for current study (2nd Column).

	Validation (from [10])	Analysis for the current study	Units
Evaporative media	CELdek5090	CELdek7060	-
Specific surface area	650	363	$m^2\ m^{-3}$
Thickness	50–150	100	mm
Frontal Area	762 × 464	650 × 506	mm^2
Air velocity	1.1 – 1.4	1.25	$m\ s^{-1}$

3.4. Hybrid evaporative-vapor compression system

The configuration for the HEVC system is similar to the one shown in Fig. 1. The outdoor air is first cooled as it passes through the evaporative cooler. The cold air is directed to the condenser of the VCC by the outdoor fan, where it absorbs the rejected heat. In our HEVC model, the dry bulb temperature at the evaporative cooler outlet is used as an input for the VCC. It is used to evaluate the condensation temperature instead of the outdoor dry bulb temperature (See Table 2). Additionally, the power consumed by the water pump in the evaporative cooler was assumed to be a constant value equal to 15 W [10]. The water pumping power was added to the total system power while calculating the COP of HEVC system.

Fig. 7 shows the resulting COPs for HEVC for a range of outdoor dry bulb temperatures and relative humidities. Additionally, Fig. 7 shows the COP of VCC without the additional evaporative cooling. The results show that the HEVC outperforms the VCC for all conditions. For a constant dry bulb temperature, the COP increases with decreasing relative humidity of outdoor air. Dry air exhibits a relatively greater mass transfer driving potential (Eq. 10) and therefore, the resulting evaporative cooling load and saturation efficiency are also higher. This trend is consistent with the findings of previous researchers on the topic [11,19]. Fig. 7 also helps explain why HEVC systems may be best suited for hot and dry climates, because that is where the performance benefits are the greatest. For example, at an outdoor dry bulb temperature equal to 55 °C and outdoor relative humidity equal to 40%, the HEVC has a 41% higher COP compared to the VCC system. Conversely, cold and humid climates may not be appropriate for adoption of HEVC systems. At an outdoor dry bulb temperature equal to 35 °C and outdoor relative humidity equal to 80%, HEVC exhibit a 6% higher COP than VCC.

3.5. Refrigerants

Eqs. 1 and 3 were developed based on a R32 compressor which had a displacement volume was equal to 18.5 cm^3. In this study, we further expanded our analysis to consider low GWP refrigerants (R32, R290, R452B, and R454B) and R410A (a common HFC refrigerant currently being used in room air conditioners). This analysis allowed us to identify the refrigerants which have comparatively favorable thermophysical properties for implementation into HEVC systems. To model the performance of other refrigerants, it is assumed that the volumetric and isentropic efficiencies of the compressor remain constant for the same indoor and outdoor climate conditions. For the given condensation and evaporation saturation temperatures, the pressure ratio for R32 is used to evaluate Eqs. 1 and 3 for all refrigerants. Eqs. 2 and 4 are then evaluated based on thermophysical properties of the refrigerant being investigated.

Additionally, the volumetric cooling capacity of the VCC changes with the change of refrigerant. To account for that, the compressor volumetric displacement was adjusted for each refrigerant until the cooling capacity of the system matched that of R32 at A-cooling condition ($T_{indoor,DB} = 26.7$ °C, $T_{outdoor,DB} = 35$ °C) from AHRI Standard 210/240 [25]. This approach has been adopted and validated by past researchers investigating the effect of refrigerant change in VCC systems

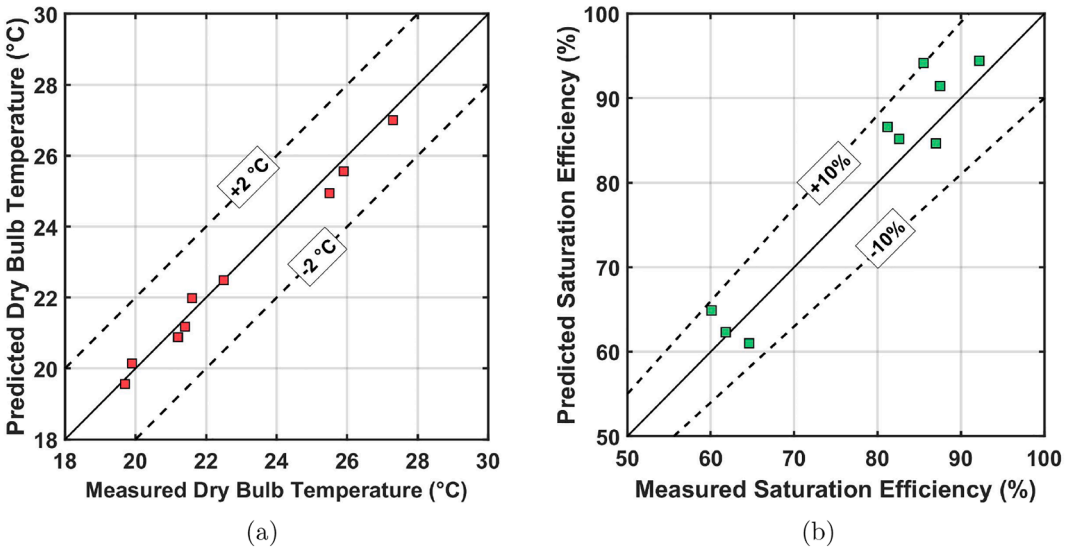

Fig. 6. A comparison of the model predictions versus measured evaporative cooling data (from [10]): (a) outlet dry bulb temperatures and (b) saturation efficiencies.

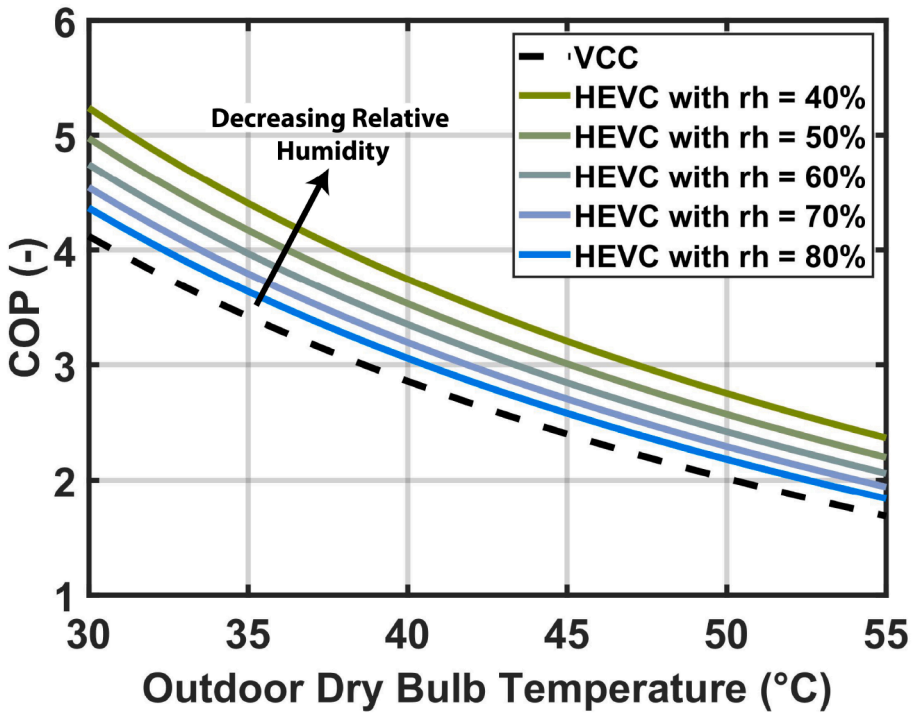

Fig. 7. A comparison of traditional VCC against HEVC at outdoor dry bulb temperatures ranging from 30 to 55 °C and relative humidities ranging from 40% to 80%.

[31,32].

4. Analysis results and discussion

4.1. HEVC versus VCC in various climates

A good agreement with the literature gave us confidence in the accuracy of the modeling approach defined in the previous section. This model was then used to investigate the feasibility of HEVC systems for cities listed in Table 1. For each city, the annual energy consumption for both VCC and HEVC systems were estimated for a 3.5 kW cooling system using ASHRAE climatic design conditions [21]. For both types of systems, the energy requirements were first evaluated on a monthly basis and then summed to evaluate the annual energy consumption. (Table 4).

Table 4
Compressor displacement volume for different refrigerants. At A-cooling condition ($T_{indoor,DB} = 26.7$ °C, $T_{outdoor,DB} = 35$ °C) AHRI Standard 210/240 [25], the corresponding cooling capacity of VCC is equal to 3.5 kW.

Refrigerant	Compressor Displacement Volume ($m^3 \times 10^{-6}$)
R32	18.5
R410A	20
R290	34
R452B	20.5
R454B	20.5

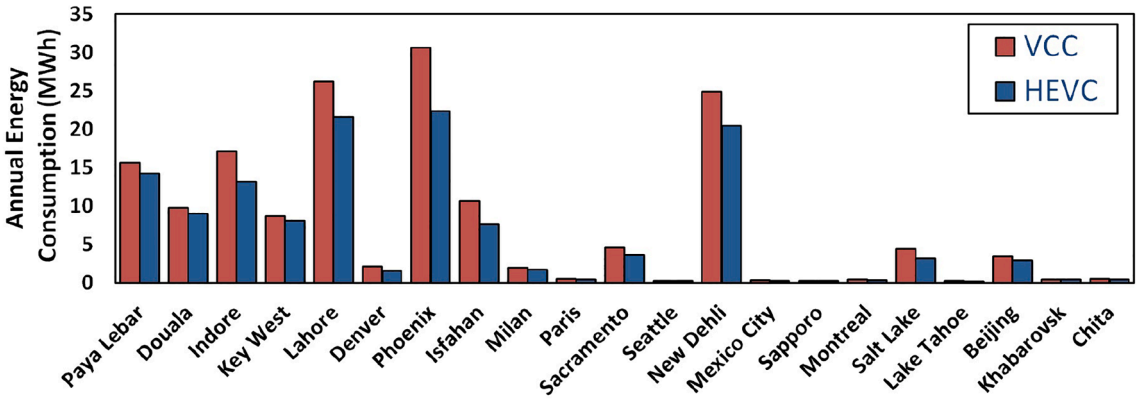

(a)

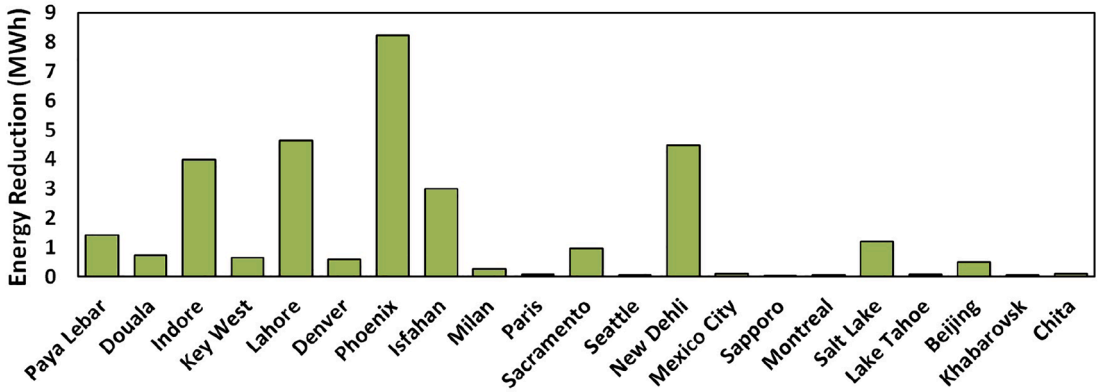

(b)

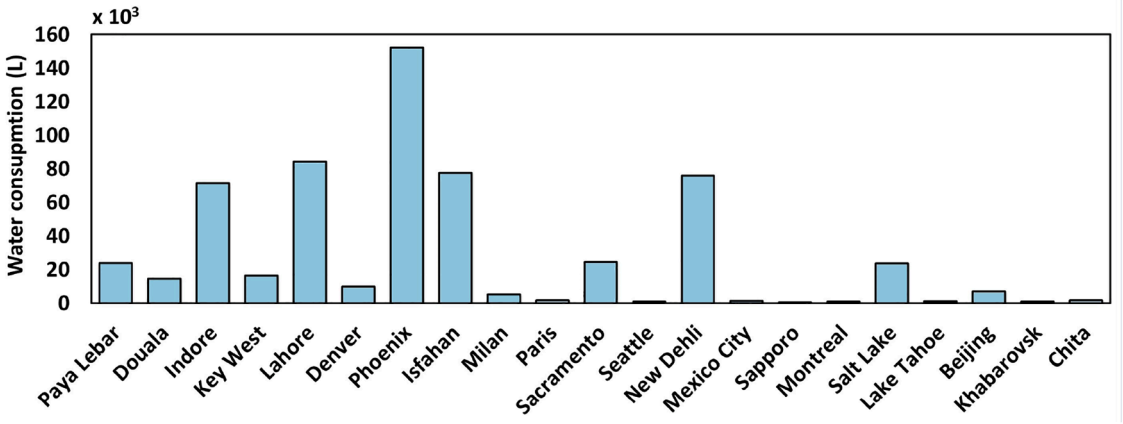

(c)

Fig. 8. (a) Annual energy consumption for HEVC versus VCC with a 3.5 KW cooling capacity. (b) Reduction in annual energy consumption for HEVC compared to VCC. (c) Annual water consumption of a HEVC system for 21 different climates from Table 1.

Fig. 8 provides a summary of the results from this study. Fig. 8(a) highlights the differences in annual energy consumption for VCC and HEVC are shown for a 3.5 kW cooling system in the 21 cities listed in Table 1, while 8(b) shows the reduction in annular energy consumption from adoption of HEVC systems. All the climates investigated in this study benefit from the adoption of HEVC technology, with at least 5% reduction in energy reduction in annual energy consumption. In particular, cities with hot arid climates (Köppen-Geiger climate classification: Bsh – Lahore, BSk – Denver, BWh – Pheonix, BWk – Isfahan) benefit the most from HEVC adoption with approximately 20% reduction in energy compared to VCC systems. Additionally, there are also energy-saving opportunities in areas that have tropical and temperate climates with dry summers (Köppen-Geiger climate classification: As – Indore, Cwa – New Dehli).

Conversely, tropical climates (Köppen-Geiger climate classification: Af – Singapore, Am – Cameroon, Aw – Key West), continental climates (Köppen-Geiger climate classification: Dfa – Sapporo, Dfb – Montreal, Dsa – Salt Lake, Dsb – Lake Tahoe, Dwa – Beijing, Dwb – Khabarovsk, Dwc – Chita) and temperate climates with no dry season (Köppen-Geiger climate classification: Cfa – Milan, Cfb – France) are not appropriate for

the adoption of HEVC technology. In these climates, which are relatively more humid, both the VCC and HEVC operate in an inefficient manner. VCC systems require additional power to meet the higher latent heat loads from dehumidification. For HEVC systems, the saturation efficiency of the evaporative cooler deteriorates with increasing outdoor humidity (See Fig. 7). Instead, alternative technologies which are capable of separate dehumidification and sensible cooling would be more appropriate for these climates [33].

Fig. 8(c) shows the annual water volume required to operate a 3.5 kW HEVC system. On average, for every kWh saved by the HEVC, 21 L of water were required for the evaporative cooling. The standard deviation was low and was equal to 3.6 L kWh^{-1}. This volume of water consumption was the greatest for Phoenix where the HEVC system would need 1.52×10^5 L to operate. For context, an average American home utilizes 522 L per day [34]. For a home in Phoenix, the addition of a 3.5 KW HEVC system would approximately result in a 80% increase in water consumption. Additionally, it also insightful to compare the HEVC water use intensity to that of thermoelectric and hydroelectric power plants, which on average utilized 49 L kWh^{-1} in 2017 [35]. In the U.S, the adoption of HEVC systems has the potential of reducing water consumption required for power generation, as well reduce the need for additional power generation. However globally, the water use intensity of power plants varies significantly depending on the available natural resources, technologies, economics, etc [36]. Thus, while HEVC is an attractive low-cost technology for meeting the global cooling demand, future policy discussions on the adoption of HEVC must weigh the energy savings against the impact on local water resources.

4.2. HEVC with low GWP refrigerants

Fig. 9 shows the percent energy reduction for HEVC systems with different refrigerant working fluids. Overall, these differences are minimal and can be explained by the differences in thermophysical properties of the refrigerants, which affect both the cooling capacity of the system and the compression work required from the compressor. Among the refrigerants considered, R290 benefits the least from adopting HEVC technology. This can be explain by the shape of its saturation curve (often referred to as liquid–vapor dome). Of particular importance is the slope of the saturation pressure with respect to the saturation temperature. In the condenser of an HEVC, a relatively high saturation pressure reduction implies lower compression work. R290 exhibits a relatively lower change in pressure with a decrease in saturation temperature. Thus, R290 shows a relatively lower enhancement compared to R32, which has the highest change in pressure with a decrease in saturation temperature.

In addition, recall from Eq. 3 that the refrigerant-side mass flow rate is a function of the refrigerant vapor suction density at the compressor inlet. In general, for a constant pressure ratio, the refrigerant mass flow rate increases with increasing vapor density. Thus, the refrigerants with a relatively higher vapor density will benefit more the adoption of HEVC system. At a constant evaporation temperature equal to 11.7°C, R290 has the lowest vapor density, while R410A has the highest (Table 5).

In addition to having lower pumping power requirements, HEVC systems also have a higher cooling capacity compared to VCC operating at the same operating conditions. This occurs due to two main reasons: 1) higher refrigerant flow rates 2) a lower thermodynamic quality at the evaporator inlet. Note the difference in State Point 4 for the two configurations in Fig. 2. The magnitude of this cooling capacity enhancement is increase is directly related to the vaporization enthalpy. A refrigerant with a high vaporization enthalpy will exhibit a higher cooling capacity increase and consequently, a higher COP. Among the refrigerants investigated, R290 had the highest vaporization enthalpy, while R410A has the minimum.

Thus, the performance of an HEVC system is a complex function of the thermophysical properties of the working fluids. Overall, R454B and R32 exhibited the greatest performance increase as a result of conversion from VCC to HEVC.

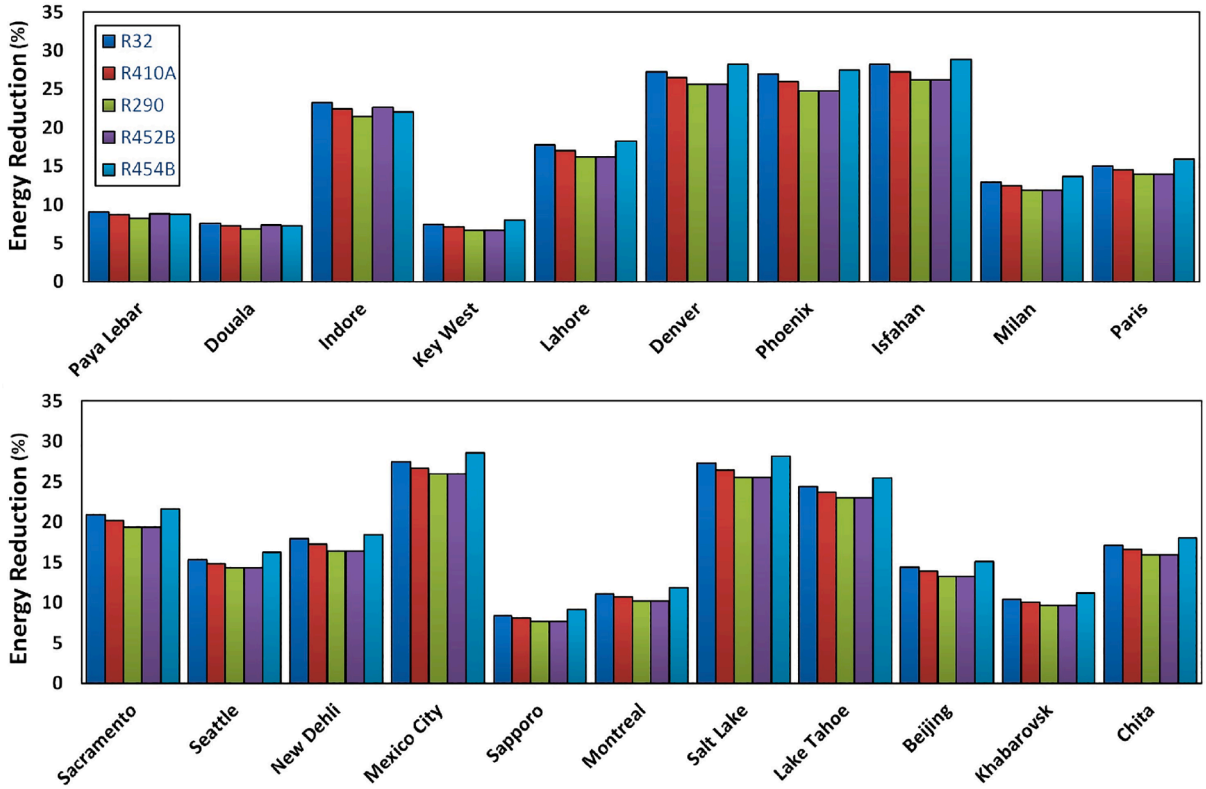

Fig. 9. A comparison of performance enhancements from refrigerants R32, R410A, R290, R452B, and R454B for 21 different climates from Table 1.

Table 5
Refrigerant properties, from [21,22].

	R32	R410A	R290	R452B	R454B
Molecular weight (kg/kmol)	52	72.6	44	63.5	62.6
ASHRAE safety class (–)	A2L	A1	A3	A2L	A2L
GWP (–)	677	1920	5	698	467
Saturation Pressure at 15 °C (kPa)	1281	1254	732	1165	1150
Vaporization enthlapy at 15 °C (kJ kg^{-1})	290	202	352	239	245
Liquid density at 15 °C (kg m^{-3})	1001	1107	507	1036	1026
Vapor density at 15 °C (kg m^{-3})	35	49	16	39	38
Saturation Pressure at 50 °C (kPa)	3520	3432	1907	3208	3165
Vaporization enthlapy at 50 °C (kJ kg^{-1})	194	122	272	155	167
Liquid density at 50 °C (kg m^{-3})	808	865	439	831	826
Vapor density at 50 °C (kg m^{-3})	115	167	44	128	123
Liquid specific heat at 50 °C (kJ $kg^{-1}K^{-1}$)	2.9	2.9	2.7	2.6	1.8
Liquid thermal conductivity at 50 °C (mW $m^{-1}K^{-1}$)	25	21	24	22	22

5. Conclusions

HEVC is a promising low-cost technology that has the potential of meeting the increasing global cooling demand while operating much more efficiently than the standard VCC. In the HEVC, an indirect evaporative cooler is used in conjunction with a VCC system. It is used to cool the air before it comes in contact with the condenser of the VCC. This allows the condenser to operate at a relatively lower temperature and thereby, reducing the compression power required.

In this paper, we developed thermodynamic models for both VCC and HEVC systems with a 3.5 kW cooling capacity. The accuracy of the modeling methodology was validated against experimental data from the literature. We then compared their performances to each other for 21 different global climates. These climates were identified based on the Köppen-Geiger climate classifications. Design conditions based on ASHRAE weather data [21] were then used as inputs to estimate the annual energy consumption for all the climates. In general, hot arid climates (Köppen-Geiger climate classifications: Bsh, BSk, BWh, BWk) benefit the most from the adoption of HEVC systems, with more than 20% reduction in energy. Tropical and temperate areas with dry summers (Köppen-Geiger climate classifications: As, Cwa) are also feasible for HEVC system. Additionally, a comparison of different low GWP refrigerant fluids in the HEVC indicates that R454B and R32 exhibit the greatest performance increase.

HEVC utilizes fresh water to cool the condenser air. Climates that benefit the most from HEVC tend to have limited freshwater resources. Thus, we also evaluated the annual water volume required to operate a 3.5 KW HEVC system. On average, 21 L of water were required to save 1 kWh. For an average American home in Arizona state (Köppen-Geiger climate classifications: BWh), that is approximately an 80% increase in household water consumption. This indicates that HEVC requires a significant amount of water and geographical policy discussions on the adoption of HEVC must be informed by their water use intensity, as well as the availability of local water resources.

CRediT authorship contribution statement

Tabeel A. Jacob: Conceptualization, Methodology, Writing - original draft. **Nihar Shah:** Supervision, Writing - review & editing. **Won Young Park:** Writing - review & editing.

Declaration of Competing Interest

The authors declare that they have no known competing financial interests or personal relationships that could have appeared to influence the work reported in this paper.

References

[1] International Energy Agency (IEA). The Future of Cooling: Opportunities for energy-efficient air conditioning. Technical report, International Energy Agency (IEA); 2018.
[2] Nihar Shah, Max Wei, Virginie Letschert, Amol Phadke. Benefits of Energy Efficient and Low-Global Warming Potential Refrigerant Cooling Equipment. Technical report, Lawrence Berkeley National Laboratory, E-Scholarship Repository, Berkeley, CA (United States); 2019.
[3] Chasik Park, Hoseong Lee, Yunho Hwang, Reinhard Radermacher. Recent advances in vapor compression cycle technologies. Int J Refrig 2015;60:118–34. doi: 10.1016/j.ijrefrig.2015.08.005.
[4] McLinden Mark O, Seeton Christopher J, Pearson Andy. New refrigerants and system configurations for vapor-compression refrigeration. Science 2020. https://doi.org/10.1126/science.abe3692.
[5] Cengel Yunus A, Boles Michael A. Thermodynamics: an engineering approach. 8th Ed. McGraw-Hill; 2015.
[6] McLinden Mark O, Steven Brown J, Brignoli Riccardo, Kazakov Andrei F, Domanski Piotr A. Limited options for low-global-warming-potential refrigerants. Nat Commun 2017;8:1–9. https://doi.org/10.1038/ncomms14476.
[7] Lee Hoseong, Troch Sarah, Hwang Yunho, Radermacher Reinhard. LCCP evaluation on various vapor compression cycle options and low GWP refrigerants. Int J Refrig 2016;70:128–37. https://doi.org/10.1016/j.ijrefrig.2016.07.003.
[8] Liu Huanwei, Zhou Qiushu, Zhao Haibo. Experimental study on cooling performance and energy saving of gas engine-driven heat pump system with evaporative condenser. Energy Conv Manage 2016;123:200–8. https://doi.org/10.1016/j.enconman.2016.06.044.
[9] José Rui Camargo, Carlos Daniel Ebinuma, José Luz Silveira. Experimental performance of a direct evaporative cooler operating during summer in a Brazilian city. Int J Refrig 2005;28(7):1124–32. doi:10.1016/j.ijrefrig.2004.12.011.
[10] Martínez P, Ruiz J, Cutillas CG, Martínez PJ, Kaiser AS, Lucas M. Experimental study on energy performance of a split air-conditioner by using variable thickness evaporative cooling pads coupled to the condenser. Appl Therm Eng 2016;105:1041–50. doi:10.1016/j.applthermaleng.2016.01.067.
[11] Tianwei Wang, Chenguang Sheng, Agwu Nnanna AG. Experimental investigation of air conditioning system using evaporative cooling condenser. Energy Build 2014;81:435–43. doi:10.1016/j.enbuild.2014.06.047.
[12] Zhang Lun, Zha Xiaobo, Song Xia, Zhang Xiaosong. Optimization analysis of a hybrid fresh air handling system based on evaporative cooling and condensation dehumidification. Energy Conv Manage 2019;180:83–93. https://doi.org/10.1016/j.enconman.2018.10.100.
[13] Dieter CA, Maupin MA, Caldwell RR, Harris MA, Ivahnenko TI, Lovelace JK, Barber NL, Linsey KS. Estimated use of water in the United States in 2015: U.S. Geological Survey Circular. Technical report, Water Availability and Use Science Program 2018.
[14] U.S. Department of Energy. Estimating Freshwater Needs to Meet Future Thermoelectric Generation Requirements. U.S. Department of Energy/National Energy Technology Laboratory (NETL); 2011.
[15] Paolo D'Odorico, Kyle Frankel Davis, Lorenzo Rosa, Carr Joel A, Davide Chiarelli, Jampel Dell'Angelo, et al.. The Global Food-Energy-Water Nexus. Rev Geophys 2018;56(3):456–531. doi:10.1029/2017RG000591.
[16] Goswami DY, Mathur GD, Kulkarni SM. Experimental Investigation of Performance of a Residential Air Conditioning System with an Evaporatively Cooled Condenser. J Solar Energy Eng 1993;115(4):206–11. https://doi.org/10.1115/1.2930051.
[17] Hajidavalloo E, Eghtedari H. Performance improvement of air-cooled refrigeration system by using evaporatively cooled air condenser. Int J Refrig 2010;33(5):982–8. doi:10.1016/j.ijrefrig.2010.02.001.
[18] Ebrahim Hajidavalloo. Application of evaporative cooling on the condenser of window-air-conditioner. Appl Therm Eng 2007;27(11–12):1937–43. doi:10.1016/j.applthermaleng.2006.12.014.
[19] Ndukaife Theodore A, Agwu Nnanna AG. Enhancement of Performance and Energy Efficiency of Air Conditioning System Using Evaporatively Cooled Condensers. Heat Transfer Eng 2019;40(3–4):375–87. https://doi.org/10.1080/01457632.2018.1429063.
[20] Peel MC, Finlayson BL, McMahon TA. Updated world map of the Köppen-Geiger climate classification. Hydrol Earth Syst Sci 2007. https://doi.org/10.5194/hess-11-1633-2007.
[21] ASHRAE. 2017 ASHRAE handbook: Fundamentals. Atlanta, GA: American Society of Heating, Refrigeration and Air-Conditioning Engineers; 2017.
[22] Klein SA. Engineering Equation Solver (EES), Version 10. F-Chart Software 2019.
[23] Li Daqing, Groll Eckhard A. Transcritical CO_2 refrigeration cycle with ejector-expansion device. Int J Refrig 2005;28(5):766–73. https://doi.org/10.1016/j.ijrefrig.2004.10.008.
[24] Domanski Piotr A, McLinden Mark O. A simplified cycle simulation model for the performance rating of refrigerants and refrigerant mixtures. Int J Refrig 1992;15(2):81–8. https://doi.org/10.1016/0140-7007(92)90031-O.
[25] ANSI/AHRI. 2008 Standard for Performance Rating of Unitary Air-Conditioning & Air-Source Heat Pump Equipment. Standard 210/240, 240; 2008.
[26] Wu JM, Huang X, Zhang H. Theoretical analysis on heat and mass transfer in a direct evaporative cooler. Appl Therm Eng 2009;29(5–6):980–4. https://doi.org/10.1016/j.applthermaleng.2008.05.016.

[27] Ali Pakari, Saud Ghani, Comparison of 1D and 3D heat and mass transfer models of a counter flow dew point evaporative cooling system: Numerical and experimental study. Int J Refrig 2019;99:114–25. doi:10.1016/j.ijrefrig.2019.01.013.
[28] Chenguang Sheng, Agwu Nnanna AG. Empirical correlation of cooling efficiency and transport phenomena of direct evaporative cooler. Appl Therm Eng 2012;40:48–55. doi:10.1016/j.applthermaleng.2012.01.052.
[29] Qun Chen, Ning Pan, Zeng-yuan Guo. A new approach to analysis and optimization of evaporative cooling system II: Applications. Energy 2011;36(5):2890–8. doi:10.1016/j.energy.2011.02.031.
[30] He Suoying, Guan Zhiqiang, Gurgenci Hal, Hooman Kamel, Yuanshen Lu, Alkhedhair Abdullah M. Experimental study of film media used for evaporative pre-cooling of air. Energy Conv Manage 2014;87:874–84. https://doi.org/10.1016/j.enconman.2014.07.084.
[31] Shen Bo, Abdelaziz Omar, Shrestha Som, Elatar Ahmed. Model-based optimizations of packaged rooftop air conditioners using low global warming potential refrigerants. Int J Refrig 2018;87:106–17. https://doi.org/10.1016/j.ijrefrig.2017.10.028.
[32] Amlaku Abie Lakew, Olav Bolland. Working fluids for low-temperature heat source. Appl Therm Eng 2010;30(10):1262–8. doi:10.1016/j.applthermaleng.2010.02.009.
[33] Gluesenkamp Kyle R, Nawaz Kashif. Separate sensible and latent cooling: Carnot limits and system taxonomy. Int J Refrig 2021;127:128–36. https://doi.org/10.1016/j.ijrefrig.2021.02.019.
[34] DeOreo William B, Mayer Peter, Kiefer Jack. Residential End Uses of Water, Version 2: Executive Report. Water Res Found 2016.
[35] U.S. Environmental Protection Agency. Water withdrawals by U.S. power plants have been declining; 2018.
[36] Yue Qin, Mueller Nathaniel D, Stefan Siebert, Jackson Robert B, Amir AghaKouchak, Zimmerman Julie B, et al.. Flexibility and intensity of global water use. Nat Sustain 2019;2(6):515–23. doi:10.1038/s41893-019-0294-2.